Research on Engineering Structures & Materials
www.jresm.org
MIM Research Group

Research Article

Performance evaluation of fly ash-based sustainable reactive powder concrete reinforced with hybrid steel–glass fibers

Nadia Salman Hussein [*,a], Hadeel K. Awad [b]

Department of Civil Engineering, University of Baghdad, Baghdad, Iraq

Article Info

Article History:

Received 04 Apr 2026

Accepted 25 May 2026

Keywords:

Reactive powder concrete;
Fly ash;
Hybrid fibers;
Mechanical properties;
Sustainability

Abstract

Reactive Powder Concrete (RPC) is a high-strength cement-based composite and low water-to-cementitious ratio; however, it is characterized by a high cement content, which raises sustainability concerns. The objectives were to produce eco-friendly products. RPC with replacing cement partially with fly ash and to optimize hybrid reinforcement with steel–glass fibers to enhance mechanical strength and, subsequently, lower environmental impacts. The fly ash replaced cement at the rate of 20%, and the total fibers were fixed at a constant of 1% by volumetric ratios of hybrid steel to glass fibers (1:0 steel, 0.75:0.25, 0.50:0.50, 0.25:0.75, and 0:1 glass). Compressive strength at 28 days, flexural, and splitting tensile strengths of the 20% fly ash with the incorporation of micro steel fibers (1%) were found to be higher than reference mix without fly ash under thermal curing increased by 4.47%, 2.39% and 2.01% respectively, In contrast, Partial replacement of steel fiber with glass fiber at different hybrid ratios The findings showed gradual compressive strength reduction (1.05–3.33%), flexural strength (1.62–17.67%), and splitting tensile strength (1.57–14.61%) as compared to control mix containing 1% micro steel fibers. Both fly ash and fiber hybridization influenced the density, water absorption, and porosity of RPC.

1. Introduction

Concrete technology has evolved rapidly into a new composite material known as Reactive Powder Concrete (RPC), which produces better structures and can be stronger than standard concrete [1]. RPC consists of extremely fine powders (Portland cement, sand, quartz powder, and silica fume). It sometimes (not always) uses steel fibers and always uses superplasticizers to reduce the water-to-cement ratio (w/c) below 0.2, and must raise the workability of RP [2]. RPC is a unique form of high-strength concrete characterized by its exceptionally high compressive strength and durability [3,4]. However, it requires a lot of cement and silica fume in its production, increasing costs and environmental impacts due to the cement industry's environmental impact [5]. Fly ash reduces the heat of hydration, improves workability, and, due to its spherical shape, decreases water demand. Fly ash enhances durability by increasing sulphate attack resistance and polishing the microstructure. Moreover, its application can significantly reduce energy consumption and CO_2 emissions during cement production [6,7]. Although RPC is a superior-performing material compared to conventional concrete, it behaves as a brittle material under tensile and compressive loading; hence, fiber reinforcement is widely used to improve toughness and post-cracking behavior [7,8]. Using Short steel fibers in concrete usually improves crack performance and post-cracking ductility, as well as the energy absorption capacity of structural elements [9]. While widely used in RPC, steel fibers are prone to corrosion when exposed to the concrete surface [10]. Glass fiber has a high potential for direct replacement of steel fiber due to its good corrosion resistance and relatively low density; a hybrid combination between the two should also be studied in RPC.

*Corresponding author: nadia.Salman2501m@coeng.uobaghdad.edu.iq
[a]orcid.org/0009-0008-8895-4541; [b]orcid.org/0009-0006-7132-125X
DOI: http://dx.doi.org/10.17515/resm2026-1602ma0404rs

Using sustainable supplementary materials in combination with glass fibers improves concrete's mechanical performance, extends its service life, and supports sustainability [6]. Nevertheless, it remains critical and a research challenge to optimize RPC to achieve both high mechanical performance and sustainability simultaneously using hybrid fiber systems in combination with supplementary cementitious materials.

Study [11] investigated the behavior of RPC incorporating single fibers (SF, GF, CF) and two hybrid fiber types (SF-GF, GF-CF, and CF-SF), keeping the fiber volume fraction constant at 2% and including a control mix. CF-RPC performed better in compressive property, while SF-RPC performed well in splitting tensile strength and flexural strength. However, CF-RPC had tensile and flexural strengths similar to those of SF-RPC but lower toughness. The hybrid combination with 1% SF and 1% CF displayed the best overall performance, whilst the fiber contribution to flexural strength ranged from 17% to 38%, which was greater than for other strength properties.

In terms of sustainability, study [7] highlighted the potential to produce sustainable RPC by replacing a portion of cement with fly ash (8, 12, 16) % and reported that 8% fly ash yielded ideal compressive strength (96.5) Mpa, (9.38) Mpa, and density (2395 kg/m3). Furthermore, study [12] demonstrated that the incorporation of micro steel fibers under warm-water curing conditions resulted in the highest compressive and flexural strengths of 138.9 MPa and 22.4 Mpa, respectively. Under these conditions, the compressive strength improved by 27.96% over that of the reference mix, and the flexural strength was also enhanced by 39.55% when micro steel fibers were blended into the mixtures. The splitting tensile strength at peak was 20.89 Mpa indicating the significant role of curing regime and fiber type in enhancing RPC performance. Additionally, study [13] examined the influence of glass fibers at volume fractions ranging from 0.1% to 0.4%, with an optimum content (0.75%). At this ideal proportion, the compressive, splitting tensile, and flexural strengths increased by 15%, 24%, and 27%, respectively, compared to plain RPC.

These results show that while individual parameters have been studied extensively, their combined influence during controlled curing remains under-researched. In general, the reviewed works show that fiber type and content have a significant effect on the mechanical behavior of RPC (especially flexural and tensile properties). Steel fibers contribute strength and toughness; their crack-bridging potential is sufficiently efficient, while glass fibers might contribute to ductility, but excessive content of them renders the mechanical performance even worse than pure concrete due to their lower stiffness and weaker interfacial bond with the matrix. In addition, the use of fly ash also contributes to sustainability. It facilitates a pozzolanic action that densifies the microstructure, but its effects are strongly dependent on replacement levels, curing conditions, and mix design.

However, the cumulative effects of mixing supplementary cementitious materials with fiber systems on structural performance have not been well assessed. In contrast, previous work has focused on only one constituent at a time. Additionally, previous studies have focused more on strength development, without providing detailed assessments of durability-related properties or of the interactions between fiber hybridization and matrix densification. Thus, the possible synergistic behavior between incumbent fly ash and hybrid steel–glass fibers with respect to crack-bridging mechanisms, ITZ refinement, and the optimal balance between strength and durability is not yet clearly understood based on laboratory experimentation, especially due to the lack of thermal curing conditions. Thus, the current study proposes a new integrated approach to concurrently investigate the combined influence of fly ash addition and steel–glass fiber hybridization on the mechanical and durability properties of RPC. Therefore, this research aims to develop sustainable RPC incorporating hybrid fibers to partially replace cement with fly ash and to evaluate mechanical properties under an accelerated-curing environment.

2. Materials and Method

2.1. Material

2.1.1 Fly Ash

Fly Ash was categorized as Class F, and the standards were established in accordance with [14]. Tables 1 and 2 present the chemical and physical properties.

Table 1. Chemical composition of fly ash [14]

Chemical composition	Results %	class F Requirement [14]
$Fe2O_3$	5.20	
$Al2O_3$	17.75	sum of value more than 50%
SiO_2	65.57	
SO_3	0.26	Maximum 5%
MgO	0.86	---
CaO	2.2	Max 18%
K2O	3.40	---
Na_2O	2.25	---
Loss. of. ignition	2.8	Max 6%

Table 2. Physical Characteristics of fly ash [14]

Physical properties	Results %	class F Requirement [14]
Maxi. amount retained on 45 μm (No. 325) sieve: 34%	26.8	Max 34%
Specific gravity	2.330	----
Surface area-(Blaine method) m^2/ Kg	610	----
Physical form	powder	----
Strength Activity Index with Portland cement at 7 days,	92	min 75

2.1.2 Cement

The OPC (CEM 1-42.5 R) cement used in the studies meets the chemical and physical characteristics outlined in [15]. Tables 3 and 4 present the properties of cement

Table3. The physical properties of the cement [15]

Physical properties	Results	Limits of [15]
Specific surface area (Blaine approach) (m^2/kg)	402.6	≥ 280
Setting time (Vicat's approach) Initial setting (min)	110	≥ 45
Setting time (Vicat's approach) Final setting time (hr)	3:25	≤ 10
Soundness by Autoclave Approach (%)	0.036 %	≤ 0.80
Compressive strength (MPa) (2) day	23.3	≥20
Compressive strength (MPa) (28) day	43	≥ 42.5

Table 4. Chemical Composition of the Cement [15,16]

Oxide Compositions	Weight (%)	Limits of [15]
L.O.I	2.815	Max (4)
Lime (CaO)	63.89	-----
Iron oxide (Fe_2O_3)	3.58	-----
Alumina (Al_2O_3)	5.40	-----
Silica (SiO_2)	18.87	-----
Magnesia (MgO)	1.84	Max (5)
Sulfate (SO_3)	2.33	SO3≤ 2.8 if C3A > 3.5 SO3≤ 2.5 if C3A ≤ 3.5
Insoluble residue (IR)	0.51	Max (1.5)
Cl^- (Chloride)	0.078	—
Major compounds of OPC		
Tri-calcium Silicate (C_3S)	68.64	Bogue equation calculation according to [16]
Di-calcium Silicate (C_2S)	2.32	
Tri-calcium Aluminate (C_3A)	8.25	
Tetra-calcium Aluminoferrite (C_4AF)	10.89	

2.1.3 Sand

Fine aggregate that passed through a 600μm sieve. Normal specifications for fine aggregate were met. [17]. The fine aggregate properties are shown in Table 5 and 6 shows the sand grading.

Table 5. Grading of fine aggregate [17]

Sieve size (mm)	Cumulative Passing %	Limits according to [17] Zone 4
10	100	100
4.75	100	95-100
2.36	100	95-100
1.18	100	90-100
0.6	100	80-100
0.3	28.1	15-50
0.15	5.4	0-15

Table 6. Physical and Chemical Characteristics of Fine Aggregates [17]

properties	Test results	Limits according to [17]
Specific gravity	2.56	------
Material Finer than 0.075 mm	2.5	Max 5%
Fineness modulus	1.67	------
Dry rodded density (kg/m^3)	1680	------
Absorption (%)	1.07	------
Sulfate content %	0.18	Max (0.5) %

2.1.4 Silica Fume

The properties and strength activity index of silica fume meet the requirements of [18], their chemical and physical characteristics are presented in Tables 7 and 8.

Table 7. Chemical composition of Silica Fume (SF) [18]

Oxide	Results %	[18] requirement
Silicon Oxide (SiO_2)	92.23	Min (85) %
Aluminum Oxide (Al_2O_3)	0.31	------
Magnesium Oxide (MgO)	0.34	------
Iron Oxide (Fe_2O_3)	1.3	------
Calcium Oxide (CaO)	2.8	------
Loss of Ignition	2.13	Max (6) %
Moisture content	0.32	Max (3) %

Table 8. Physical Requirements of Silica Fume (SF) [18]

Physical properties	Test results	[18] requirement
State	Amorphous powder with submicron particle size	-
Retained on 45 µm (No.325) sieve (%)	7.1	≤ 10
Accelerated Pozzolanic Strength Activities Index with the OPC at 7 days, min percent of control	111.4	Min (105)
Specific Surface (m2/g)	17	≥ 15

2.1.5 Water

Tap water for mixing is suitable [19].

2.1.6 Superplasticizer

Hyperplast PC800M-type G (water-reducing, high-range, and retarding admixtures) having a density of 1.070 ± 0.02 g/cm3. The superplasticizer was used at a dosage of 0.5 - 3.5 % by weight of the total cementitious materials and having a pH of (5–7), in compliance with [20].

2.1.7 Micro steel fiber

A straight micro steel fiber with a nominal diameter of 0.2 mm and length of 13 mm was employed in this study, providing an aspect ratio for the fiber (l/d) = l/d=65 and density 7860 Kg/m3. Tensile Strength 2600 MPa

2.1.8 Glass fiber

The used glass fibers were alkaline-resistant, measuring 12 mm in length, to ensure good resistance in the alkaline cementitious matrix. The fibers had a 14 μm (0.014 mm) diameter, which translates to an aspect ratio of 80. and density 2680 Kg/m3. Tensile Strength 1700 MPa

2.2. Design and Mixes

The mixtures were designed using the methods of [21,22], and trial The mixes were prepared for verification. the reference (R1S) a mixture without replacement and five fly ash–based mixes (20% cement substitution) ,A 20% fly ash replacement was selected based on previous studies and trial mixes, as it provides an optimal balance between strength and microstructural enhancement[36].. The micro steel fiber volume fraction was fixed at 1% to maintain workability and ensure uniform dispersion, based on previous studies. [7,22], and progressively replaced with glass fibers at volume fractions of 0.25, 0.50, 0.75, and 1.00. The dosage of superplasticizer was adjusted to maintain the desired flow. All mixtures were designed using a fixed water-to-cementitious materials ratio (w/cm) of 0.21 (Fig. 1). The selected materials are presented. The flowability was regulated with the flow table test based on [23], achieving a value of (110 ± 5 mm) as specified by [24]. the measured flow values of the control and another RPC mixtures ranged from 105mm to 113 mm (Fig. 2). The proportions of the mixtures are summarized in Table 9.

Fig. 1. Materials used in the trial mixes of RPC

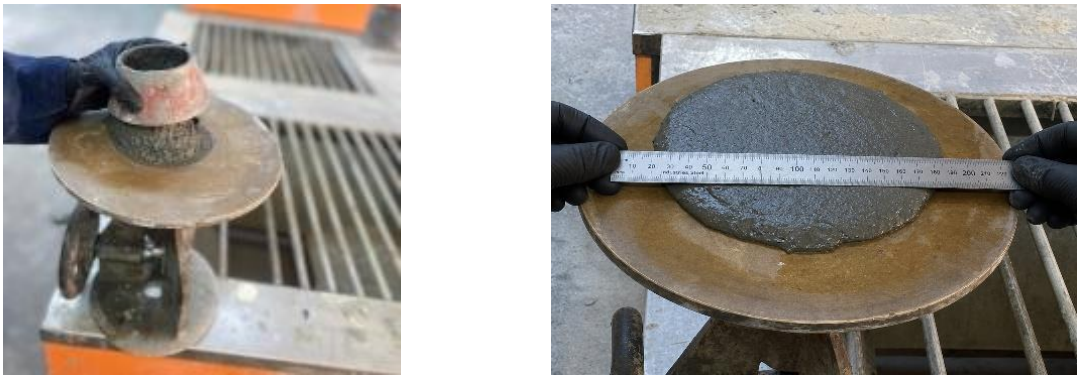

Fig. 2. Flow table test procedure

2.3. Mixing and Casting

The mixing process was performed according to the procedure suggested by [2]: Cement, fly ash, and silica fume were initially dry-mixed for about 3 minutes to achieve homogeneous distribution. Sand was added and mixed for another 5 minutes. the superplasticizer was diluted in a small amount of water before mixing, and during mixing, the water–superplasticizer solution was added to the mixture; the mixture was then mixed for 3 minutes. The parts not reached by the mixer were mixed by hand. The mixer was run for an additional 5 minutes to achieve adequate fluidity. Micro steel and glass fibers were homogeneously dispersed into the mix at 3 min; thereafter, the mixing process continued for the remaining 2 min. Overall, mixing one batch takes about 15 minutes from adding water to completion.

Table 9. Mix proportions of RPC for 1 m^3 (kg/m^3) [21,22]

Mixes	Cement	Sand	Silica Fume	Fly Ash	w/Cm	water	*sp l/m^3	** Micro Steel fiber	** Glass fiber
R1S	920	1015	230	------	0.21	242	21.85	79	------
RF1S	736	1015	230	184	0.21	242	20.70	79	------
RF0.75S+0.25G	736	1015	230	184	0.21	242	21.50	59	7
RF0.50S+0.50G	736	1015	230	184	0.21	242	21.85	39	13
RF0.25S+0.75G	736	1015	230	184	0.21	242	22.31	20	20
RF1G	736	1015	230	184	0.21	242	22.89	------	27

*Note: * 1.8 - 1.99 % by weight of the total cementitious materials, ** fiber% by volume of mixes*

2.4. Curing

The normal curing of RPC results in a slower rate of strength development than that observed with heat or steam curing, in which temperature is the main controlling factor [25, 26]. Immediately after mixing, the fresh concrete was cast into steel molds and vibrated in place before covering with nylon sheets and demolding 24 h later; specimens were heat-cured in water using the following schedule: temperature increased from 20 °C to 70 °C at a rate of 20 °C/h, followed by maintenance at 70 °C for 5 h/day for three days; specimens were then cured with water at 20 °C until tested [27]. The thermal-curing procedure used in this study is illustrated in (Fig. 3).

Fig. 3. Hot-water curing of RPC specimens at 70 °C (5 h/day for 3 days), followed by water curing at 20 °C

2.5. Testing

2.5.1. Fresh density test

Fresh density of RPC is determined in accordance with [28], using a known-mass-and-volume cylinder. The fresh density was calculated based on Eq. (1);

$$D_f = \frac{M_c - M_m}{V_m} \quad (1)$$

where: D_f is the fresh density of concrete (kg/m^3), Mc is the mass of the cylinder filled with fresh concrete (kg), Mm is the mass of the empty cylinder (kg), and Vm is the volume of the cylinder (m^3).

2.5.2. Compressive Strength

The compressive strength of RPC (50 × 50 × 50 mm) was determined according to [24], using three cube specimens cured for 7 and 28 days. The reported compressive strength values are averages of the three specimens tested at each age. Compressive strength was calculated using Eq. (2), as illustrated in (Fig. 4.)

$$fc = \frac{P}{Ac} \tag{2}$$

where: fc: Compressive Strength (MPa), P: Maximum applied load (N), Ac: Cross-section area (mm^2).

Fig. 4. Testing and failure of the specimens

2.5.3. Flexural Strength

Three prismatic specimens (50 × 50 × 250 mm) according to the specifications presented in [29], were tested at curing ages of 7 and 28 days. Values reported for flexural strength are average test results of three specimens at each age. The flexural strength was determined with Eq. (3), as illustrated in (Fig 5).

$$R = \frac{3pl}{2bd^2} \tag{3}$$

Where: R -The flexural value is denoted by the letter (MPa), P -Maximum load is denoted by (N), L-stands for the span's length (mm), b -average width of specimen in millimeters (mm),d -stands for the average prism thickness depth (mm).

Fig 5. Testing and failure of the specimens

2.5.4. Splitting Tensile Strength Test

The splitting tensile strength (100 × 200 mm) according to [30], with dimensions at the curing ages of 7 and 28 days. The RPC was tested on three cylindrical specimens. Except where specified, values reported are the average of three specimens per age. Eq. (4), as illustrated in (Fig. 6).

$$fsp = \frac{2p}{\pi dl} \quad (4)$$

where: fsp- Indirect tensile strength (MPa), p- Max. Applied load indicated by the testing machine (N), d-Cylinder diameter (mm), l-Cylinder length (mm).

Fig. 6. Testing and failure of the specimens

2.5.5. Dry Density Test

The density of RPC was determined in accordance with [31]. Three cubes with dimensions of (50 × 50 × 50 mm) were tested at 28 days. The density was calculated using the formula as given in Eq. (5);

$$D = \frac{M}{V} \quad (5)$$

where: D -is the density of the specimen in (kg/ m^3), M- is the dry mass of the specimen in (kg), V- is the volume of the specimen in (m^3)

2.5.6. Water Absorption and Voids Test

Water absorption and voids tests were conducted at 28 days following [32], computed from the mean of three specimens. The water absorption ratio was calculated using Eq (6), and the void content was calculated using Eq (7);

$$Absorption\% = \frac{B - A}{A} * 100 \quad (6)$$

Where: A- Oven dry weight (g), B- Saturated surface dry weight (g).

$$Voids\% = \frac{w2 - w1}{w2 - w3} \quad (7)$$

Where: w1- The sample mass is oven-dried in the air, w2- The mass of the sample is surface dried in the air after being submerged in water, w3- The mass of the sample in the water

3. Results and Discussion

3.1. Dry and Fresh Density

The fresh and dry densities of the RPC mixtures are shown in Table 10 and (Fig. 7), respectively. The mixture without fly ash (R1S) shows the highest fresh density of 2515 kg/m^3. The density of the fresh mix decreased slightly with the addition of fly ash because fly ash has a lower specific gravity than cement [33], which increases the paste volume and lowers the overall mixture's mass. The highest dry density was 2683 kg/m^3 from RF1S, and the lowest was 2627 kg/m^3 from RF1G. The reduction in density of RPC mixtures is due not only to the lower density of glass fibers compared with micro-steel fibers, but also to differences in fiber stiffness and dispersion, which may lead to slight increases in entrapped air and localized voids within the matrix. Overall, the

addition of fly ash and the partial substitution of micro-steel fibers with glass fibers led to a decrease in fresh density; however, dry density increased due to a reduction in air and pore volume entrapped in the matrix [33]. The reason for this was attributed to the pozzolanic reactions of fly ash with cement that produce denser and amorphous C–S–H gel, reducing porosity as well as lessening the number and length of micro-cracks, thereby improving the bond strength within the concrete matrix, leading to a higher density structure than that observed for reference samples [7].

Table 10. Results of Fresh and Dry Density (kg/m^3)

Mixes	Fresh Density (kg/m^3)	Dry Density (kg/m^3) at 28 days
R1S	2515	2645
RF1S	2506	2683
RF0.75 S+0.25 G	2493	2669
RF0.50 S+0.50 G	2480	2655
RF0.25 S+0.75 G	2467	2641
RF1G	2454	2627

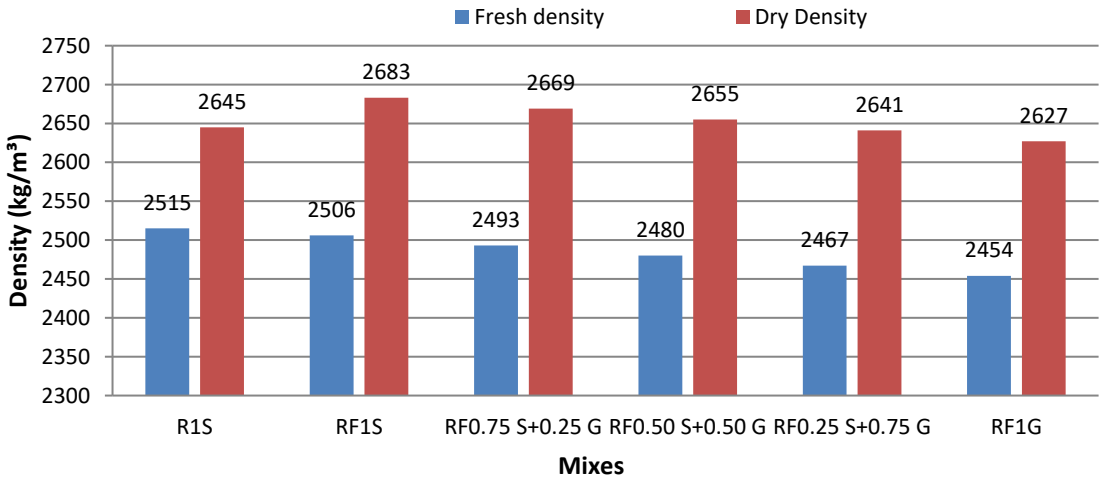

Fig 7. Fresh and Dry density of reference and sustainable mixes

3.2. Water Absorption and Porosity

Water absorption and porosity at 28 days are shown in Table 11 and (Fig. 8). The lowest values corresponded to RF1S (0.114% and 1.75). The reason for the decrease in the size of the pores is a result of filling and the high pozzolanic activity of fly [33], which contributes to microstructural densification. Fine fly ash particles improve particle packing by filling micro-voids between the cement grains and, during the secondary pozzolanic reaction, produce more C–S–H gel, giving longer bonds, and refining the pore structure rather than just reducing total porosity. With increasing glass fiber content, water absorption and porosity both increased slowly and reached maximum values (0.148% and 2.25%) at RF1G.

Table 11. Results of Water absorption and Porosity %

Mixes	Water absorption at 28 days (%)	Porosity at 28 days (%)
R1S	0.124	1.90
RF1S	0.114	1.75
RF0.75 S+0.25 G	0.121	1.86
RF0.50 S+0.50 G	0.130	2.00
RF0.25 S+0.75 G	0.139	2.12
RF1G	0.148	2.25

This behavior indicates an increased porosity due to lower density of glass fiber and their relatively weaker fiber–matrix bonding as glass, which may lead to the formation of micro-voids around the fibers. This finding agrees with that of [34]. exhibited that higher glass fiber contents led to a lower compactness rate of the matrix and a larger connectivity ratio of pores. In general, the new pore structure when fly ash is added to all specimens results in lower capillary porosity and finer pore size distribution; on the other hand, improve of microstructure with increased glass fiber content is attributed to a more porous ITZ and more void formation.

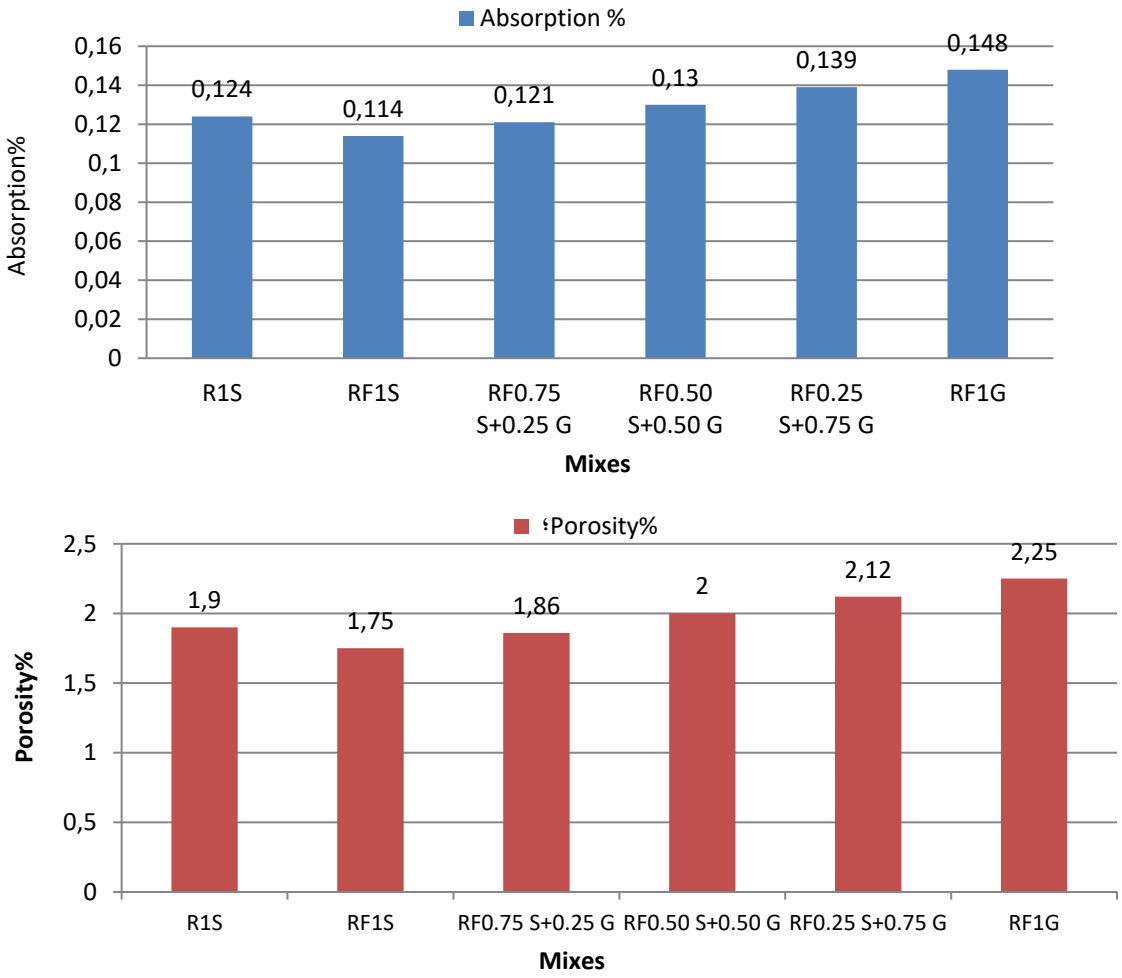

Fig. 8. Water absorption and porosity of reference and sustainable mixes

3.3. Compressive Strength

Compressive strength of RPC at both 7 and 28 days gradually decreased when micro steel fibers were substituted with glass fibers. The incorporation of 20% cement substitution with fly ash and 1% micro steel fibers (RF1S) resulted in the highest compressive strengths at both 7 days and 28 days, 101.32 MPa (+3.39%) and 119.10 MPa (+4.47%), respectively, relative to the reference mixture. Due to the pozzolanic reactivity of fly ash, it can react with the calcium hydroxide (CH) generated by cement hydration to form more Calcium silicate hydrate (C–S–H). As a result, this reaction helps produce a denser microstructure and lower porosity in the concrete matrix, which, in turn, increases its strength [7,33].

The presence of discrete steel fibers in the RPC matrix which, in turn, delays crack propagation and thereby enhances compressive strength, unlike glass fibers, which were less effective in this regard. as illustrated in Table 12 and (Fig. 9). On the contrary, replacing steel fibers with glass fibers caused higher decrease in compressive strength where the explanation for this behavior may be due to their lower elastic modulus and high smooth surface which cause a weak interfacial bonding. Additionally, fiber dispersion and the possibility of interfacial micro-voids can affect local stress concentrations, thereby degrading the compressive strength.

To conclude, fly ash addition combined with steel fiber reinforcement serves to improve the microstructure of RPC. However, the reduction in compressive strength decreases gradually with increasing glass fiber content in aggregates, because this mechanism is less energy-efficient than the agglomeration mechanism for controlling crack coalescence. The results are analogous to the reported finding by [34].

This is shown by the error bars (i.e., low variability in the experimental results). As shown in the mean Bonferroni and the corresponding error bars, slight overlap of some error bars is observed; however, differences between mixtures were greater than their respective standard deviation values, clearly demonstrating that the variation represents a statistically significant result rather than experimental error. The standard deviation (≈1.30–1.50 MPa) also confirms good repeatability.

Table 12. Results of compressive (MPa)

Mixes	Compressive Strength (MPa)				Percentage change relative to reference mix (R1S) (%)	
	7 days	Std. Dev	28 days	Std. Dev	7 days	28 days
R1S	98.00	1.41	114.00	1.41	0.00	0.00
RF1S	101.32	1.45	119.10	1.37	+3.39	+4.47
RF0.75 S+0.25 G	99.95	1.30	117.95	1.46	+1.99	+3.47
RF0.50 S+0.50 G	97.60	1.41	115.60	1.46	−0.41	+1.40
RF0.25 S+0.75 G	94.85	1.35	112.80	1.50	−3.21	−1.05
RF1G	92.10	1.31	110.20	1.37	−6.02	−3.33

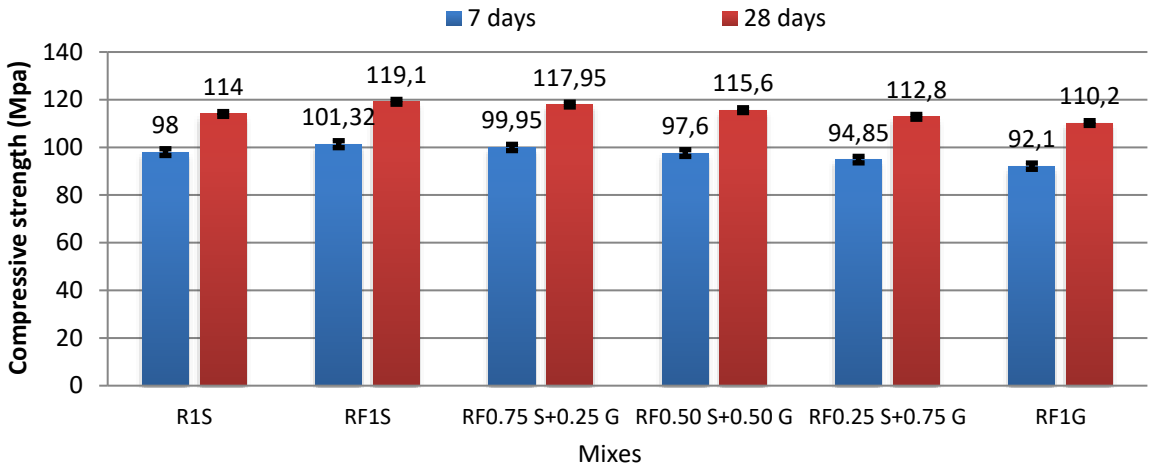

Fig 9. Influence of fiber on the compressive strength of RPC

3.4. Flexural Strength

The flexural strength of RPC decreased gradually as micro steel fibers were replaced by glass fibers at 7 and 28 days, in different percentages. The maximum flexural strength was recorded in the reference mix with 1% micro steel fibers, and higher glass fiber content resulted in lower flexural strength. As the main role is in controlling FRC cracking, and modifying the response of the material after matrix cracking has occurred, by bridging over these cracks and thereby giving some post-cracking ductility [35], By investigation, it will be noted that micro steel fibers represent better crack-bridging efficiency than SF because of its higher elastic modulus, tensile strength and rough surface texture which can combine with enhanced mechanical interlocking and fiber–matrix bond. This leads to better stress transmission at the crack, increased fracture toughness, and improved post-fracture ductility. In contrast, the flexural rigidity of glass fiber is low due to its smooth surfaces, which limit interaction with the polymer matrix and interfacial adhesive bond, and its limited crack-bridging capacity or septa. The faster inherent increase in the calculated crack-

opening displacement causes early premature crack propagation or decreases the flexural strength. The use of steel fibers leads to more effective load transfer across cracks and higher post-cracking in RPC compared with glass fiber**,** due to the high tensile strength, as is illustrated in Table 13 and (Fig**.** 10). The findings are consistent with the findings presented by [11]. Extremely low standard deviation (≈0.14–0.23 MPa) demonstrated very good consistency. The decrease in strength by these values is greater than that corresponding to the range of variability, indicating that fiber hybridization has a large effect.

Table 13. Results of Flexural strength (MPa)

Mixes	Flexural strength (MPa)				Percentage change relative to reference mix (R1S) (%)	
	7 days	Std. Dev	28 days	Std. Dev	7 days	28 days
R1S	8.97	0.15	10.47	0.15	0.00	0.00
RF1S	9.12	0.15	10.72	0.15	+1.67%	+2.39
RF0.75 S+0.25 G	8.76	0.14	10.30	0.2	-2.34%	-1.62
RF0.50 S+0.50 G	8.17	0.15	9.60	0.2	-8.92%	-8.31
RF0.25 S+0.75 G	7.58	0.17	8.91	0.21	-15.50%	-14.90
RF1G	7.33	0.17	8.62	0.23	-18.28%	-17.67

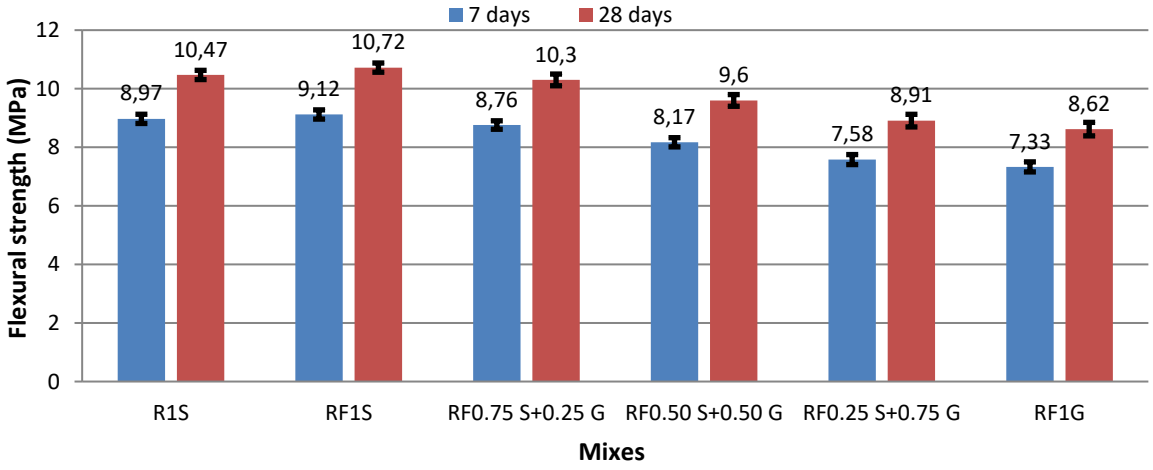

Fig. 10. Influence of fiber on the flexural strength of RPC mixtures

3.5. Splitting Tensile Strength Test

The splitting tensile strength of RPC decreased gradually with increasing glass fiber replacement ratios on days 7 and 28, respectively. With a lower concentration of glass fibers. References with 1% micro steel fibers; whereas, the lowest values were observed in mixes with a higher volume percentage of glass fiber. In this assessment, fiber slippage is proposed as an indicator of tensile failure occurred due to weak bonding between the glass fibers and the RPC. This was likely due to inadequate chemical treatment of the fiber surface, which is required to develop an appropriate structural texture that enables it to withstand high tensile loads and stresses within the RPC matrix. [34], which outlined that the contribution of fibers to improve tensile properties is dominantly influenced by bonding characteristics and surface characteristics. The results indicated that steel fibers provide better tensile reinforcement for RPC, resulting in stronger fiber–matrix bonding and improved crack bridging. In contrast, a higher glass fiber content harms tensile performance owing to weaker fiber-matrix interactions and increased interfacial defects. The results are consistent with data reported by [11]. The small standard deviation (≈0.12–0.15 MPa) indicates high precision

and repeatability. The differences between the mixes are larger than experimental error, confirming statistical significance

Table 14. Results of Splitting tensile strength (MPa)

Mixes	Splitting tensile strength (MPa)				Percentage change relative to reference mix (R1S) (%)	
	7 days	Std. Dev	28 days	Std. Dev	7 days	28 days
R1S	7.80	0.13	8.90	0.13	0.00	0.00
RF1S	7.92	0.15	9.05	0.13	+1.54%	+1.69%
RF0.75 S+0.25 G	7.65	0.132	8.76	0.14	−1.92%	−1.57%
RF0.50 S+0.50 G	7.30	0.13	8.37	0.15	−6.41%	−5.96%
RF0.25 S+0.75 G	6.90	0.13	7.94	0.12	−11.54%	−10.79%
RF1G	6.64	0.12	7.60	0.13	−14.87%	−14.61%

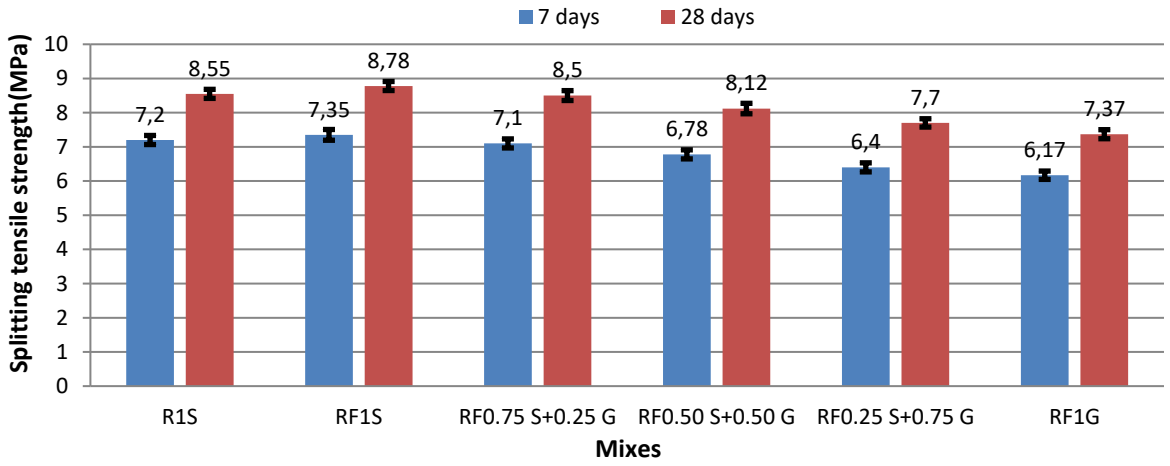

Fig. 11. Effect of fiber on the splitting tensile strength of RPC mixtures

4. Conclusions

- This study provides unique scientific insight into how the utilization of fly ash and hybridization with steel–glass fibers in thermal curing regimes interact, as previous studies have not fully addressed this topic or its impact on the degree of sustainability benefits and mechanical behavior.
- It accelerates the pozzolanic reactions mainly by improving cement hydration and fly ash reactivity, resulting in rapid C–S–H formation and early densification of the matrix. This agrees with the improvement of mechanical strength at 20% fly ash replacement level.
- Replacing 20% of the cement with fly ash improved the mechanical behavior of reactive powder concrete (RPC) cured at elevated temperatures. The compressive strength increased by 4.47% at 28 days compared with the control mixture, while the flexural and splitting tensile strengths increased by 2.39% and 1.69%, respectively. This improvement can be attributed to the micro-filling effect and secondary pozzolanic reactions of fly ash, which enhance matrix densification, refine the pore structure, and enhance the interfacial transition zone (ITZ).
- Gradually replacing micro steel fibers with glass fibers affected the strength performance of RPC. For steel-to-glass hybrid ratios of 0.75:0.25, 0.50:0.50, 0.25:0.75, and 0:1, the compressive strength changed by +3.47%, +1.40%, −1.05%, and −3.33%, respectively. Flexural and splitting tensile strengths declined with increasing glass fiber content. Optimum mechanical performance was achieved with fly ash and 1% micro steel fibers. In contrast, higher glass fiber contents led to progressive strength reduction due to their lower stiffness and weaker crack-bridging capability than steel fibers. For flexural loading, the effect is

greater as it controls crack propagation and the fiber-bridging mechanism of failure. This is also related to the fact that the interfacial transition zone (ITZ) between glass fibers and the cement matrix is weaker, resulting in easier fiber pull-out and, therefore, less effective crack-bridging by glass fibers than by steel fibers.

- Fiber hybridization had a greater impact on flexural and splitting tensile strengths than on compressive strength. This indicates that flexural performance, which is mainly an interfacial mechanism originating in fiber-reinforcement crack-bridging in the matrix phase of concrete, was more affected by fiber type than by compressive strength, compared with reference steel fibers. The decrease in flexural strength with increasing glass fiber content can be attributed to lower stiffness and fiber bonding of glass fibers compared to steel fibers.
- Fresh density decreased due to the use of fly ash and glass fibers, but the dry density increased slightly during matrix densification. The water absorption and porosity increased with the addition of glass fiber, which may be related to weaker fiber–matrix bonding and less efficient fiber dispersion. This is associated with increased micro voids and less efficient particle packing, resulting in a more porous microstructure.
- Overall, incorporating 20% fly ash enhances RPC performance while reducing cement consumption. Although hybrid fiber systems exhibit lower strength than steel fiber reinforcement at higher glass contents, they may offer improved durability due to glass fibers' corrosion resistance. Depending on the fiber composition, this reveals a mechanical performance-versus-long-term durability trade-off.

References

[1] Nafees A, Javed MF, Musarat MA, Ali M, Aslam F, Vatin NI. FE modelling and analysis of beam column joint using reactive powder concrete. Crystals. 2021;11(11):1372. https://doi.org/10.3390/cryst11111372

[2] Danha LS, Khalil WI, Al-Hassani HM. Mechanical properties of reactive powder concrete (RPC) with various steel fiber and silica fume contents. Eng Technol J. 2013;31(16):3090–3108.

[3] Qasim RM, Aljalawi NMF. The effect of different curing temperatures on properties of reactive powder concrete reinforced by micro steel fibers. J Eng. 2024;30(6):57–66. https://doi.org/10.31026/j.eng.2024.06.06

[4] Majeed WZ, Aboud RK, Naji NB, Mohammed SD. Investigation of the impact of glass waste in reactive powder concrete on attenuation properties for Bremsstrahlung ray. East Eur J Phys. 2023;1:102–108. https://doi.org/10.26565/2312-4334-2023-1-12

[5] Wong LS. Durability performance of geopolymer concrete: A review. Polymers. 2022;14(5):868. https://doi.org/10.3390/polym14050868

[6] Zaid O, Ahmad J, Siddique MS, Aslam F, Alabduljabbar H, Khedher KM. A step towards sustainable glass fiber reinforced concrete utilizing silica fume and waste coconut shell aggregate. Sci Rep. 2021;11(1):12822. https://doi.org/10.1038/s41598-021-92228-6

[7] Muhsin ZF, Fawzi NM. Effect of fly ash on some properties of reactive powder concrete. J Eng. 2021;27(11):32–46. https://doi.org/10.31026/j.eng.2021.11.03

[8] Xu J, Wu C, Xiang H, Su Y, Li ZX, Fang Q, et al. Behaviour of ultra-high performance fiber reinforced concrete columns subjected to blast loading. Eng Struct. 2016;118:97–107. https://doi.org/10.1016/j.engstruct.2016.03.048

[9] Awad HK. Influence of cooling methods on the behavior of reactive powder concrete exposed to fire flame effect. Fibers. 2020;8(3):19. https://doi.org/10.3390/fib8030019

[10] Li F, Lv T, Wei S. Performance, mechanical properties and durability of a new type of UHPC—basalt fiber reinforced reactive powder concrete: A review. Polymers. 2023;15(14):3129. https://doi.org/10.3390/polym15143129

[11] Raza SS, Qureshi LA, Ali B, Raza A, Khan MM, Salahuddin H. Mechanical properties of hybrid steel–glass fiber-reinforced reactive powder concrete after exposure to elevated temperatures. Arab J Sci Eng. 2020;45(5):4285–4300. https://doi.org/10.1007/s13369-019-04164-4

[12] Luti AA, Abbas ZK. The effect of different curing methods on the properties of reactive powder concrete reinforced with various fibers. Eng Technol Appl Sci Res. 2024;14(3):14225–14232. https://doi.org/10.48084/etasr.7177

[13] Ambika GM, Mani SC, Saraswathi SGV, Palanisamy S. Evaluation of reactive powder concrete mechanical, durability, and microstructural properties under various exposure conditions. Matéria. 2025;30:e20250222. https://doi.org/10.1590/1517-7076-rmat-2025-0222

[14] ASTM International. Standard specification for coal fly ash and natural pozzolan (ASTM C618-25a). 2025.

[15] Central Organization for Standardization and Quality Control (COSQC). IQS 5: Portland cement – first update. Baghdad; 2019.
[16] ASTM International. Standard specification for Portland cement (ASTM C150/C150M-24). 2024.
[17] Central Organization for Standardization and Quality Control (COSQC). IQS No. 45: Natural aggregates for concrete. Baghdad; 1984.
[18] ASTM International. Standard specification for silica fume used in cementitious mixtures (ASTM C1240-20). 2020.
[19] Central Organization for Standardization and Quality Control (COSQC). IQS No. 1703: Water used for concrete and mortar. Baghdad; 2018.
[20] ASTM International. Standard specification for chemical admixtures for concrete (ASTM C494/C494M-24). 2024.
[21] Richard P, Cheyrezy M. Composition of reactive powder concretes. Cem Concr Res. 1995;25(7):1501–1511. https://doi.org/10.1016/0008-8846(95)00144-2
[22] Hussain ZA, Aljalawi NMF. Behavior of reactive powder concrete containing recycled glass powder reinforced by steel fiber. J Mech Behav Mater. 2022;31(1):233–239. https://doi.org/10.1515/jmbm-2022-0025
[23] ASTM International. Standard test method for flow of hydraulic cement mortar (ASTM C1437-20). 2020.
[24] ASTM International. Standard test method for compressive strength of hydraulic cement mortars (ASTM C109/C109M-24). 2024.
[25] Luti AA, Abbas ZK. The investigation of different curing regimes on reactive powder concrete strength: A review. J Eng. 2024;30(11):200–208. https://doi.org/10.31026/j.eng.2024.11.12
[26] Hendi SI, Aljalawi NM. Effect of various curing regimes on some properties of reactive powder concrete (RPC). J Eng. 2024;30(11):21–34. https://doi.org/10.31026/j.eng.2024.11.02
[27] ACI Committee 517. Accelerated curing of concrete at atmospheric pressure (ACI 517.2R-92). USA; 2017.
[28] ASTM International. Standard test method for density (unit weight), yield, and air content of concrete (ASTM C138/C138M-17a). 2017.
[29] ASTM International. Standard test method for flexural strength of concrete (ASTM C293-19). 2019.
[30] ASTM International. Standard test method for splitting tensile strength of cylindrical concrete specimens (ASTM C496/C496M-17). 2017.
[31] Iraqi Guidelines. The concrete tests and test methods to measure density of hardened concrete. Baghdad; 2000.
[32] ASTM International. Standard test method for density, absorption, and voids in hardened concrete (ASTM C642-21). 2021.
[33] Long G, Wang X, Xie Y. Very-high-performance concrete with ultrafine powders. Cem Concr Res. 2002;32(4):601–605. https://doi.org/10.1016/S0008-8846(01)00732-3
[34] Algburi AHM, Sheikh MN, Hadi MNS. Mechanical properties of steel, glass, and hybrid fiber reinforced reactive powder concrete. Front Struct Civ Eng. 2019;13(4):998–1006. https://doi.org/10.1007/s11709-019-0533-7
[35] Bentur A, Mindess S. Fibre reinforced cementitious composites. CRC Press; 2006.
[36] Yigiter H, Aydın S, Yazıcı H, Yardımcı MY. Mechanical performance of low cement reactive powder concrete (LCRPC). *Composites Part B: Engineering*. 2012;43(7):2907–2914. https://doi.org/10.1016/j.compositesb.2012.07.042